

Effects of focused ion beam milling on the nanomechanical behavior of a molybdenum-alloy single crystal

H. Bei^{a)} and S. Shim

Department of Materials Science and Engineering, The University of Tennessee, Knoxville, Tennessee 37996, USA and Materials Science and Technology Division, Oak Ridge National Laboratory, Oak Ridge, Tennessee 37831, USA

M. K. Miller

Materials Science and Technology Division, Oak Ridge National Laboratory, Oak Ridge, Tennessee 37831, USA

G. M. Pharr and E. P. George

Department of Materials Science and Engineering, The University of Tennessee, Knoxville, Tennessee 37996, USA and Materials Science and Technology Division, Oak Ridge National Laboratory, Oak Ridge, Tennessee 37831, USA

(Received 20 July 2007; accepted 24 August 2007; published online 14 September 2007)

Nanoindentation was performed on a Mo-alloy single crystal to investigate effects of focused ion beam (FIB) milling on mechanical behavior. On a non-FIB-milled surface, pop-ins were observed on all load-displacement curves corresponding to a transition from elastic to plastic deformation. Similar pop-ins were not detected on surfaces subjected to FIB milling. This difference indicates that FIB milling introduces damage that obviates the need for dislocation nucleation during subsequent deformation. A second effect of FIB milling is that it increased the surface hardness. Together, these effects could be the source of the size effects reported in the literature on micropillar tests. © 2007 American Institute of Physics. [DOI: 10.1063/1.2784948]

The phenomenon of increasing strength with decreasing volume of material tested (size effect) has attracted much attention during the past decade. In many cases, the increase in strength results from plastic strain gradients¹ imposed during testing, e.g., in nanoindentation,²⁻⁴ microtorsion,⁵ and microbend experiments,⁶ and is attributable to the hardening caused by geometrically necessary dislocations.⁷ In order to minimize strain-gradient effects, compression tests of micropillars have been employed in recent years to explore small-scale plasticity.⁸⁻¹⁴ In these experiments, cylindrical micropillars with diameters down to hundreds of nanometers are fabricated, most often by the use of focused ion beam (FIB) milling.⁸⁻¹²

Micropillars fabricated from single-phase metals by FIB milling have shown a strong size effect, with their yield and/or flow strengths increasing with decreasing pillar sizes.⁸⁻¹² However, none of the measurements have come close to the theoretical strength, even though some of the pillar diameters were small enough (submicron) that they would be expected to contain few or no dislocations. A possible source of this discrepancy is the damaged layer that is produced during FIB milling, including a region of high dislocation density near the surface.¹⁵ These preexisting dislocations would be expected to lower the yield stress of the micropillars to a value significantly below the theoretical stress. To investigate this possibility, we recently tested Mo-alloy single crystal micropillars prepared by a technique that did not involve FIB milling.¹⁴ Interestingly, our micropillars all yielded at shear strengths close to the theoretical $\sim G/25$. The sizes of our micropillars (~ 360 – 1000 nm) are comparable to those of some of the FIB-milled pillars reported in the literature⁸⁻¹² suggesting that defects introduced during

FIB milling may have been responsible for their lower strengths.

Dislocations are not the only defects introduced during FIB milling by Ga ions. Microstructural examination by transmission electron microscopy,^{15,16} x rays,¹⁷ and atom probe tomography¹⁸ have revealed that Ga ion implantation, amorphization, and intermetallic formation can occur in a layer adjacent to the milled surface. Although the thickness of the damaged layer depends on material and experimental conditions, the thicknesses reported in the literature^{15,16,18,19} generally range from ~ 10 to 100 nm. Therefore, compression tests of micropillars fabricated by FIB milling, rather than measuring the intrinsic properties of a material, may measure the composite mechanical response of a material and its FIB-modified surface. Moreover, the influence of this damaged surface layer increases with decreasing specimen size. Hence, characterizing the effects of the FIB damaged layer on mechanical properties is important in interpreting the results of micropillar tests.

To evaluate the effects of the FIB damaged layer on mechanical properties, we conducted nanoindentation experiments on a Mo-alloy single crystal before and after FIB milling of the surface. An electrochemically polished Mo-alloy (100) single crystal having the composition Mo-(3 at. %)Nb was our starting material. Four trenches with dimensions of $70 \times 70 \times 0.1 \mu\text{m}^3$ were milled on the polished face of the Mo-alloy crystal using different accelerating voltages and currents, as listed in Table I. For a given volume of material removed, the FIB milling is faster at higher beam voltages and currents. Nanoindentation experiments were conducted at 100 different locations on each of the five regions (four FIB milled and one electrochemically polished) using a Nanoindenter XP equipped with a Berkovich diamond indenter. Load (P) and displacement (h) were

^{a)}Electronic mail: bei@ornl.gov

TABLE I. FIB conditions used in this study to mill trenches measuring $70 \times 70 \times 0.1 \mu\text{m}^3$ on an electropolished surface of a Mo-alloy single crystal.

	Beam voltage (kV)	Beam current (nA)	Time (min)
1	30	7.0	7.8
2	20	5.3	10.3
3	10	2.6	21.0
4	5	1.4	39.0

continuously recorded up to a prescribed maximum load (P_{max}) of 1.5 mN at a constant P/\dot{P} of 0.05 s^{-1} , where P is the loading rate. The area function of the indenter was carefully calibrated using standard fused silica and tungsten samples as described elsewhere.^{20,21} It was found that the shape of the indenter tip is well described as a sphere with a radius of 178 nm for indentation depths less than 20 nm.

A typical loading and unloading P - h plot for the as-polished Mo-alloy single crystal is shown in Fig. 1. Sudden displacement excursions (pop-in events) were observed during loading in all 100 tests, with the first pop-in on this particular loading curve occurring at a load of about 0.32 mN. The pop-ins are very reproducible: 90% of the pop-in loads fall within a narrow range from 0.30 to 0.34 mN.

Following previous work,²¹ we start with the assumption that the deformation prior to the first pop-in is perfectly elastic and evaluate whether this is valid here. The fully elastic P - h relationship is generally described by the Hertzian solution,²²

$$P = \frac{4}{3} E_r \sqrt{R} h^{1.5}, \quad (1)$$

where R is the radius of the indenter tip, and the reduced modulus $E_r = 1 / \{ [(1 - \nu_i^2) / E_i] + [(1 - \nu_s^2) / E_s] \}$, with E_s , ν_s , E_i , and ν_i are Young's moduli and Poisson's ratios of the specimen and indenter, respectively. For a diamond indenter, the

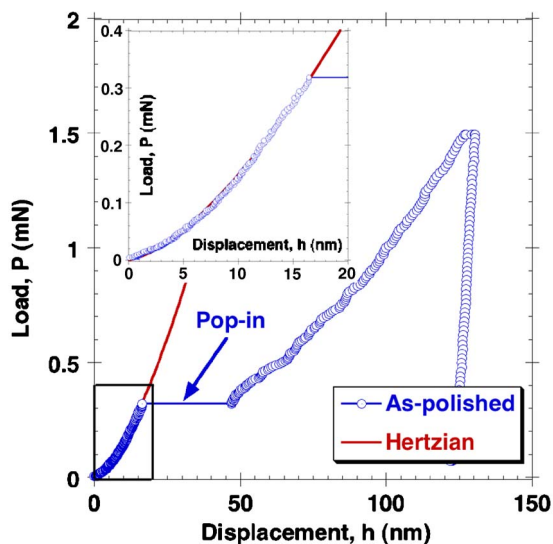


FIG. 1. (Color online) Nanoindentation results for electrochemically polished Mo-alloy single crystal: measured load-displacement curve showing pop-in during loading and calculated elastic Hertzian solution showing good agreement with experimental data before the pop-in event.

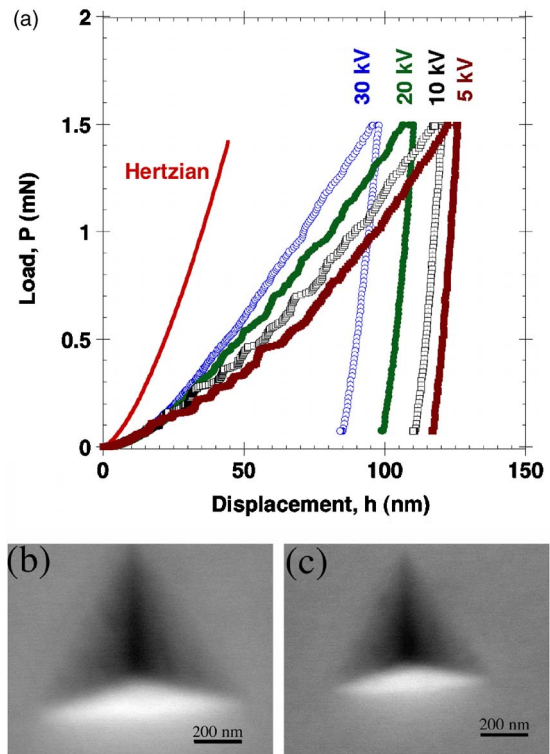


FIG. 2. (Color online) (a) Load-displacement curves from nanoindentation on surfaces prepared by focused ion beam milling. (b) and (c) are indent impressions on surfaces milled at 5 and 30 kV, respectively.

relevant elastic constants are $E_i = 1141 \text{ GPa}$ and $\nu_i = 0.07$.²³ For our Mo-alloy specimen (Mo-3Nb) we use the elastic constants of pure Mo, $E_s = 322 \text{ GPa}$ and $\nu_s = 0.3$.²⁴ By substituting these values and $R = 178 \text{ nm}$ into Eq. (1) we obtain the load-displacement behavior, which is plotted in Fig. 1 and labeled as “Hertzian.” The close agreement between the experimental data for our electropolished Mo-alloy single crystal and the Hertzian solution demonstrates that its deformation is perfectly elastic up to the first pop-in and plastic beyond that. Consistent with this, the critical resolved shear stress at the pop-in load, calculated as before^{20,21} using Hertzian analysis, was found to be 16.3 GPa ($\sim G/8$), which is close to the estimated theoretical shear stress.

Typical load-displacement curves obtained during nanoindentation on surfaces subjected to FIB milling at 5–30 kV are shown in Fig. 2(a). The same Hertzian solution as shown in Fig. 1 is also included for comparison. An obvious difference between Figs. 1 and 2(a) is that elastic-plastic transitions (large pop-in events) are not observed in the FIB-milled specimens. Although only one P - h curve from each of the FIB-milled surfaces is shown in Fig. 2(a), the lack of pop-ins indicative of elastic plastic transitions is a common feature of all nanoindentations performed. This is consistent with the notion that dislocations exist in or near the FIB-modified layer and, therefore, do not have to be nucleated at relatively high stresses. Rather, plastic deformation occurs almost from the start of nanoindentation at very small loads as indicated by the deviations of the P - h curves from the elastic Hertzian solution.

The hardness and modulus of the electrochemically polished and FIB-milled Mo-alloy surfaces were computed using the Oliver-Pharr method²³ at the maximum applied load of 1.5 mN (corresponding to indentation depths of 70–130 nm), and the results are shown in Fig. 3. FIB milling

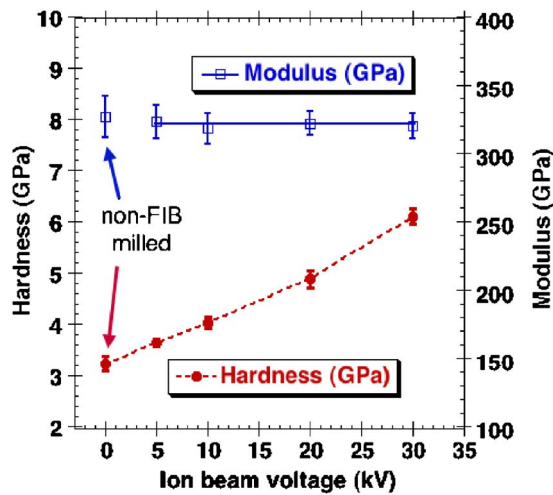


FIG. 3. (Color online) Measured hardness and modulus of Mo-alloy single crystal at maximum applied load of 1.5 mN in the electrochemically polished condition (0 kV) and after FIB milling at different ion beam voltages: hardness increases with increasing beam voltage, but modulus remains unchanged.

does not change the modulus, but increases the hardness (FIB-induced hardening). It should be noted that the hardnesses in Fig. 3 most likely underestimate the true hardness of the FIB-damaged layer due to substrate influences on the hardness measurement.²⁵ It should also be noted that the thickness and hardness of the damaged layer may depend on the angle of incidence of the ion beam relative to the milled surface.¹⁵ Decreasing the Ga ion acceleration voltage decreases the magnitude of the measured hardness. Consistent with this, the penetration depths of the indenter decrease with increasing acceleration voltage and the indent impression made on the 5 kV FIB milled surface is larger than that on the 30 kV surface [Figs. 2(b) and 2(c)].

FIB milling is being increasingly used to machine microsamples for various tests (e.g., bend, compression) in a variety of materials, including crystalline metals,^{8–12,26} metallic glasses,²⁷ and semiconductors.²⁸ Our present results raise important questions about the suitability of FIB milling as a fabrication process to make small specimens for mechanical tests. As shown above, FIB milling can introduce dislocations into the materials, which may explain why the theoretical strength is achieved in non-FIB machined samples¹⁴ but not in any of the FIB-fabricated micropillars,^{8–12} even though several of the latter are smaller than the whiskers which were shown decades ago to have strengths approaching the theoretical.²⁹

Another important question raised by the FIB-induced hardening observed here is whether the size effect reported in FIB-machined micropillars is an artifact. In a micropillar compression test, the FIB damaged layer may be harder than the underlying material, in which case it would increase the strength of the pillar. That the measured strength increases with decreasing pillar diameter would then simply be a consequence of the increasing volume fraction of the FIB damaged layer with decreasing pillar diameter. In order to cor-

rectly interpret the mechanical behavior of small specimens prepared by FIB milling, one should carefully characterize the FIB damaged layer, including its microstructure, properties, and interactions with the underlying base material, as well as investigate how to eliminate the effects of the damaged surface layer.

This research was sponsored by the U.S. Department of Energy, Division of Materials Sciences and Engineering (H.B. and E.P.G.), by the Assistant Secretary for Energy Efficiency and Renewable Energy, Office of FreedomCAR and Vehicle Technologies, as part of the High Temperature Materials Laboratory User Program (S.S.), and by the SHaRE User Facility, Division of Scientific User Facilities (M.K.M. and G.M.P.).

¹H. Gao, Y. Huang, W. D. Nix, and J. W. Hutchinson, *J. Mech. Phys. Solids* **47**, 1239 (1999).

²K. W. McElhane, J. J. Vlassak, and W. D. Nix, *J. Mater. Res.* **13**, 1300 (1998).

³W. D. Nix and H. J. Gao, *J. Mech. Phys. Solids* **46**, 411 (1998).

⁴J. G. Swadener, E. P. George, and G. M. Pharr, *J. Mech. Phys. Solids* **50**, 681 (2002).

⁵N. A. Fleck, G. M. Muller, M. F. Ashby, and J. W. Hutchinson, *Acta Metall. Mater.* **42**, 475 (1994).

⁶J. S. Stolken and A. G. Evans, *Acta Mater.* **46**, 5109 (1998).

⁷M. F. Ashby, *Philos. Mag.* **21**, 399 (1970).

⁸M. D. Uchic, D. M. Dimiduk, J. N. Florando, and W. D. Nix, *Science* **305**, 986 (2004).

⁹D. M. Dimiduk, M. D. Uchic, and T. A. Parthasarathy, *Acta Mater.* **53**, 4065 (2005).

¹⁰J. R. Greer, W. C. Oliver, and W. D. Nix, *Acta Mater.* **53**, 1821 (2005).

¹¹J. R. Greer, W. C. Oliver, and W. D. Nix, *Acta Mater.* **54**, 1705 (2006).

¹²C. A. Volkert and E. T. Lilleodden, *Philos. Mag.* **86**, 5567 (2006).

¹³B. E. Schuster, Q. Wei, H. Zhang, and K. T. Ramesh, *Appl. Phys. Lett.* **88**, 103112 (2006).

¹⁴H. Bei, S. Shim, E. P. George, M. K. Miller, E. G. Herbert, and G. M. Pharr, *Scr. Mater.* **57**, 397 (2007).

¹⁵D. Kiener, C. Motz, M. Rester, M. Jenko, and G. Dehm, *Mater. Sci. Eng., A* **459**, 262 (2007).

¹⁶J. P. McCaffrey, M. W. Phaneuf, and L. D. Madsen, *Ultramicroscopy* **87**, 97 (2001).

¹⁷R. Maass, D. Grolimund, S. V. Petegem, M. Willmann, M. Jensen, H. V. Swygenhova, T. Lehnert, M. A. M. Gijss, C. A. Volkert, E. T. Lilleodden, and R. Schwaiger, *Appl. Phys. Lett.* **89**, 151905 (2006).

¹⁸K. Thompson, D. Lawrence, D. J. Larson, J. D. Olson, T. F. Kelly, and B. Gorman, *Ultramicroscopy* **107**, 131 (2007).

¹⁹J. Mayer, L. A. Giannuzzi, T. Kamino, and J. Michael, *MRS Bull.* **32**, 400 (2007).

²⁰H. Bei, Z. P. Lu, and E. P. George, *Phys. Rev. Lett.* **93**, 125504 (2004).

²¹H. Bei, E. P. George, J. L. Hay, and G. M. Pharr, *Phys. Rev. Lett.* **95**, 045501 (2005).

²²K. L. Johnson, *Contact Mechanics* (Cambridge University, Cambridge, UK, 1985), pp. 90–93.

²³W. C. Oliver and G. M. Pharr, *J. Mater. Res.* **7**, 1564 (1992).

²⁴G. Simmons and H. Wang, *Single Crystal Elastic Constants and Calculated Aggregate Properties: A Handbook*, 2nd edition (MIT, Cambridge, MA, 1971), p. 217.

²⁵T. Y. Tsui, J. Vlassak, and W. D. Nix, *J. Mater. Res.* **14**, 2204 (1999).

²⁶C. Motz, T. Schoberl, and R. Pippan, *Acta Mater.* **53**, 4269 (2005).

²⁷B. E. Schuster, Q. Wei, M. H. Ervin, S. O. Hruszkewycz, M. K. Miller, T. C. Hufnagel, and K. T. Ramesh, *Scr. Mater.* **57**, 517 (2007).

²⁸J. Michler, K. Wasmer, S. Meier, F. Ostlund, and K. Leifer, *Appl. Phys. Lett.* **90**, 043123 (2007).

²⁹S. S. Brenner, *J. Appl. Phys.* **27**, 1484 (1956).